CNIC-01020
ZZU-0001

中国核科技报告

CHINA NUCLEAR SCIENCE AND TECHNOLOGY REPORT

粘土和仿古瓷的穆斯堡尔实验

THE MÖSSBAUER EXPERIMENT ON THE CLAYS AND THE IMITATIVE ANCIENT PORCELAINS

中国核情报中心
原子能出版社

China Nuclear Information Centre
Atomic Energy Press

高正耀：郑州大学教授，1962 年毕业于北京大学技术物理系核物理专业。

Gao Zhengyao: Professor of Zhengzhou University. Graduated from Department of Technological Physics, Peking University in 1962, majoring in nuclear physics.

CNIC-01020
ZZU-0001

粘土和仿古瓷的穆斯堡尔实验

高正耀

（郑州大学物理工程学院）

陈松华

（郑州大学电子工程系）

摘　要

分析了几种著名的古窑遗址粘土烧制过程中穆斯堡尔参数随烧制温度，烧制时间和烧制气氛的变化规律。详细研究了仿古天青汝瓷釉的穆斯堡尔参数随烧制条件的变化。穆斯堡尔谱显示天青釉含有三种铁矿物，即结构铁（Fe^{2+}和Fe^{3+}），Fe_2O_3和Fe_3O_4。随着温度的增加，顺磁峰Fe^{2+}的相对强度增加，磁性峰的磁比率减小。讨论了天青釉在烧制过程中发生的相变。还研究了天青釉的着色机理和烧制过程的磁性变化。研究了在液氦温度下天青釉超精细相互作用参数的变化和参数变化的机制。穆斯堡尔谱显示在仿古蓝钧瓷的釉料和胎料中含有Fe_2O_3、Fe_3O_4和结构铁。釉料在烧制过程中明显地经历了脱水、脱羟基、玻璃化和再结晶过程。胎料的顺磁峰二价铁的四极分裂值在烧制温度较低时就比较大，脱水和脱羟基的差别不明显，对釉料和胎料在烧制过程中磁性的变化和天蓝钧瓷的呈色机理进行了分析。

THE MÖSSBAUER EXPERIMENT ON THE CLAYS AND THE IMITATIVE ANCIENT PORCELAINS

Gao Zhengyao
(PHYSICS ENGINEERING INSTITUTE
OF ZHENGZHOU UNIVERSITY)
Chen Songhua
(ELECTRONIC ENGINEERING DEPARTMENT
OF ZHENGZHOU UNIVERSITY)

ABSTRACT

It is analyzed that Mössbauer parameter variations of clays from the famous sites of ancient kilns change with firing temperature, firing time and firing atmosphere in firing process. The variation of the Mössbauer parameters of the imitative ancient Chinese Ru porcelain sky-green glaze with the firing conditions is studied in detail. The Mössbauer spectra show that the sky-green glaze contains three kinds of iron minerals, i. e. the structural iron (Fe^{2+} and Fe^{3+}); Fe_2O_3 and Fe_3O_4. The relative intensity of the paramagnetic peak Fe^{2+} increases and the magnetic ratio of the magnetic peak decreases with increasing temperature. Based on the variation of the quadrupole splitting (QS) of the paramagnetic peak Fe^{2+}, the phase transformation characteristics of the sky-green glaze in the firing process is discussed. The coloring mechanism of the sky-green glaze and the variation of its magnetism in the firing process are also investigated. The variation of the hyperfine interaction parameters and the variable mechanism of the sky-green glaze at liquid helium temperature is studied. Mössbauer spectra of the imitative ancient blue Jun porcelain indicate that the glaze and boby materials contain Fe_2O_3, Fe_3O_4 and structural iron. It is clear that during the firing process, the glaze undergoes dehydration, dehydroxylation, vitrification and recrystallization. The Fe^{2+} quadrupole splitting value of the paramagnetic peak of the body material is rather high even at low firing temperature. The distinction between dehydration and dehydroxylation is not clear. The changes of magnetism of the glaze and body materials in the firing process and coloring mechanism of the sky-blue Jun porcelain are analyzed.

INTRODUCTION

Mössbauer effect can be utilized to trace the phase transformation of clay and glaze raw materials during firing process. The iron mineral components of some clays and imitative ancient Chinese porcelain glaze are analyzed by Mössbauer effect. The phase transition process and its characteristics of the clays and imitative ancient Chinese porcelain during the firing process are studied. Ru porcelain, Jun porcelain and Guan porcelain started from Chinese Tang Dynasty, prospered in Chinese Song Dynasty and declined in Yuan Dynasty. The technology was lost in the late years of Yuan Dynasty. The imitative ancient Chinese porcelains have been made after 1950 in Yuzhou, Ruzhou and Jingdezhen and so on. The productions of the imitative ancient porcelain were mainly relying on the porcelain makers' experience, were short of foundational study. Mössbauer study of firing process of the two imitative ancient Chinese porcelain glaze raw materials is profitable for the investigation of the ancient porcelain and the imitative ancient porcelain.

1 SPECIMENS SURVEY

The specimens condition is shown in Table 1 and Table 2.

Table 1 The specimens condition of the clays from the famous site of ancient Chinese kilns

Serial No.	Name	Time	Site
C_1	Lishan clay	1989	Xian Lishan, the raw material of terra-cotta figures of warriors and horse form the grave site of the First Emperor
C_2	Qingliangsi clay	1987	Qingliangsi in Baofeng Country, the clay from the site of the ancient Ru kiln
C_3	Xiaohuangye clay	1987	Gongxian, the clay from the site of ancient Tangsancai kiln
C_4	Dahuangye clay	1987	Gongxian, the clay from the site of ancient Tangsancai kiln

Table 2 The specimens of the imitative ancient porcelain raw material

Serial No.	Name	Time	Site
IR	The glaze material of the imitative ancient Ru porcelain	1991	Ru Porcelain Arts and Crafts Experiment Factory of Ruzhou City
IJ_1	The glaze material of the imitative ancient Jun porcelain	1991	Shenhou Town of Yuzhou City
IJ_2	The body material of the imitative ancient Jun porcelain	1991	Shenhou Town of Yuzhou City

2 EXPERIMENTAL METHODS

2.1 Firing clays

The four samples (C_1, C_2, C_3 and C_4) are fired in electric furnace in oxidizing atmosphere (in air) at different temperatures and for different time.

2.2 Firing glaze materials of the imitative ancient porcelain

The specimens of Sky-green glaze material of the imitative ancient Ru porcelain (IR), Sky-blue glaze material of the imitative ancient Jun porcelain (IJ_1) and body material of the imitative ancient Jun porcelain (IJ_2) were fired in an electrical furnace in a reductive atmosphere. The atmosphere is a mixture of C, CO, CO_2, H_2, N_2 and vapour. The firing temperature range is 300～1250℃. The temperature is kept constant at each chosen piont for 6 h and then allowed to cool down naturally. A radiation source of ^{57}Co (Pd) was used. The transmission spectra of the above specimens are measured. The Spectra were computer-fitted to a least-squares Lorentzian function. The isomeric shift (IS) is with respect to α-Fe.

2.3 Measuring low temperature spectrum of sky-green glaze material of imitative ancient Ru porcelain

The acquisition of low temperture spectrum requires the cooling of both radiation source and specimen absorber to liquid helium temperature. The mechanical fixture for driving the radiation source to make Doppler movement is a perpendicularly vibrating device. Transmission spectra at 4.2 K are measured. The radiation source used is ^{57}Co (Rh). α-Fe is used in speed calibration. The spectrum is computer-fitted to a leastsquares Lorentzian function.

3 EXPERIMENTAL RESULTS

3.1 The variation of Mössbauer parameters of the clays with firing conditions

The room temperature Mössbauer spertra of sample C_1 at different firing temperatures (after 8 h firing) are shown in Fig. 1.

3.1.1 Unfired clays

The spectra of unfired clays are obviously composed of three parts: paramagnetic Fe^{3+} doublet, Fe^{2+} doublet and sextet of magnetic component (M) (to see Table 3 and Fig. 1). The isomeric shift (IS), quadrupole splitting (QS) of paramagnetic peak Fe^{3+} and Fe^{2+}, the intensity (H) of internal magnetic field of magnetic peak are similar basically for different clays. The ratios of average values of intensities (%) of the three parts for specimens of C_1, C_2, C_3 and C_4 are Fe^{3+} : Fe^{2+} : M = 66 : 18 : 16. There may be various iron minerals in unfired clay, e.g., hematite (Fe_2O_3), magnetite ($FeO \cdot Fe_2O_3$), limonite ($Fe_2O_3 \cdot 2Fe(OH)$), siderite ($FeCO_3$), lepidocrocite (FeOOH), FeS_2 and Fe_2SO_4, etc. The size of the small parti-

cles of the iron oxides or hydroxides are usually of 10.0 nm order. The small particles have superparamagnetic relaxation effect. The particles may generate superparamagnetic doublet. Some of the iron in the form of Fe^{3+} and Fe^{2+} combines into clay minerals. The iron ions are incorporated into lattice of the clay minerals. We term it structural iron. The structural irons generate Fe^{3+} and Fe^{2+} paramagnetic doublet. The superparamagnetic doublet of the iron minerals and paramagnetic doublet of the structural iron are overlapped in the spectra at room temperature. Therefore, there are the contributions both of the small particles of iron oxides and of the structural iron in central doublet at room temperature. It is difficult to differentiate the two subspectra at room temperature. These two spectra can be distinguished by comparison between room temperature and liquid helium temperature spectra of clay[1]. The ratios of values of intensities of the Fe^{3+}, Fe^{2+} and M may be judging basis for firing atmosphere of ancient ceramic.

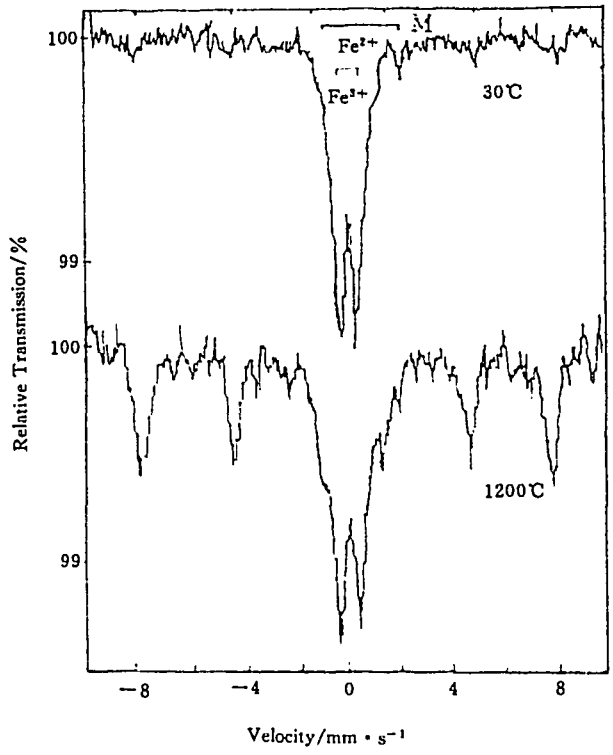

Fig. 1 The room temperature Mössbauer spectra of sample C_1 at different firing temperatures (after 8 h firing)

Table 3 Room temperature Mössbauar parameters of unfired samples C_1, C_2, C_3 and C_4

sample	Fe^{3+}			Fe^{2+}			M			
	I. S mm • s⁻¹	Q. S mm • s⁻¹	I %	I. S mm • s⁻¹	Q. S mm • s⁻¹	I %	I. S mm • s⁻¹	Q. S mm • s⁻¹	H *	I %
C_1	0.345	0.666	79.7	1.055	2.876	7.2	0.376	−0.298	499	13.1
C_2	0.341	0.648	68.1	1.064	2.731	11.4	0.315	−0.112	506	20.5
C_3	0.327	0.669	60.0	1.081	2.708	28.9	0.333	−0.166	498	11.1
C_4	0.297	0.670	57.5	1.021	2.752	24.8	0.350	−0.171	508	17.7

* H Unit in k (1000/4 π) A/m.

3. 1. 2 Physical and chemical changes and the characteristics of Mössbauer spectra of the firing clay

Mössbauer parameters of specimens C_1, C_2 at RT versus firing temperature and firing time are shown as Table 4 and Table 5.

Table 4 Room temperature Mössbauar parameters of sample C_1 vs. firing temperature and time

$\frac{T}{℃}$	$\frac{t}{h}$	Fe^{3+}			Fe^{2+}			M			
		I. S $mm \cdot s^{-1}$	Q. S $mm \cdot s^{-1}$	$\frac{I}{\%}$	I. S $mm \cdot s^{-1}$	Q. S $mm \cdot s^{-1}$	$\frac{I}{\%}$	I. S $mm \cdot s^{-1}$	Q. S $mm \cdot s^{-1}$	$\frac{H}{*}$	$\frac{I}{\%}$
200		0.297	0.697	77.0	0.968	2.733	7.9	0.303	−0.225	500	15.0
400		0.346	0.835	78.2	0.900	2.552	3.9	0.343	−0.125	497	17.9
500		0.372	1.034	80.7	0.826	2.560	1.9	0.421	−0.289	501	17.4
600		0.342	1.148	73.7	0.563	2.399	2.1	0.354	−0.266	500	24.1
700		0.382	1.208	68.9				0.302	−0.270	507	31.0
800	8	0.276	1.120	55.5				0.283	−0.144	495	44.5
850		0.320	0.963	48.8				0.354	−0.213	500	51.2
900		0.201	0.756	44.4				0.284	−0.251	499	55.6
1000		0.302	0.766	40.3				0.390	−0.191	494	57.9
1100		0.271	0.780	38.5				0.348	−0.203	499	61.5
1200		0.294	0.768	41.9				0.361	−0.228	487	58.1
	1	0.368	0.818	73.7	0.868	2.634	4.3	0.420	−0.126	511	22.0
	4	0.352	0.812	79.7	0.895	2.666	2.9	0.371	−0.213	501	17.4
400	8	0.346	0.835	78.2	0.900	2.552	3.9	0.343	−0.125	497	17.9
	12	0.397	0.876	75.3	1.066	2.997	1.7	0.399	−0.139	508	23.0
	16	0.350	0.833	75.0	0.547	2.120	1.4	0.357	−0.253	501	23.6
	1	0.344	1.095	71.5	0.651	2.494	2.7	0.324	−0.294	499	25.9
	4	0.356	1.130	73.0	0.477	2.399	2.7	0.332	−0.230	502	24.3
600	8	0.342	1.148	73.7	0.563	2.399	2.1	0.354	−0.266	500	24.2
	12	0.340	1.186	68.2	0.435	2.267	3.8	0.385	−0.304	501	27.9
	16	0.359	1.133	69.0	0.610	2.827	1.2	0.362	−0.274	506	29.8
	1	0.265	1.129	60.6				0.292	−0.214	494	39.6
	4	0.295	1.152	59.9				0.331	−0.223	501	40.1
800	8	0.276	1.120	55.5				0.283	−0.144	495	44.5
	12	0.254	1.132	53.6				0.304	−0.257	499	46.4
	16	0.308	1.120	53.8				0.363	−0.257	496	46.2
	1	0.273	0.766	42.3				0.354	−0.207	501	57.7
	4	0.215	0.766	40.3				0.290	−0.226	496	59.7
1000	8	0.302	0.749	42.1				0.390	−0.191	494	57.9
	12	0.369	0.763	39.5				0.452	−0.213	496	60.5
	16	0.203	0.764	37.3				0.296	−0.188	496	62.7

* H Unit in k (1000/4 π) A/m.

Table 5 Room temperature Mössbauar parameters of sample C_2 vs. firing temperature and time

$\frac{T}{℃}$	$\frac{t}{h}$	Fe^{3+}			Fe^{2+}			M			
		I. S $mm \cdot s^{-1}$	Q. S $mm \cdot s^{-1}$	$\frac{I}{\%}$	I. S $mm \cdot s^{-1}$	Q. S $mm \cdot s^{-1}$	$\frac{I}{\%}$	I. S $mm \cdot s^{-1}$	Q. S $mm \cdot s^{-1}$	$\frac{H}{*}$	$\frac{I}{\%}$
200		0.360	0.679	77.6	1.149	2.884	6.6	0.339	−0.092	504	15.8
400		0.368	0.813	71.4	1.017	2.868	5.1	0.423	−0.262	502	23.5
500		0.377	0.990	70.2	0.844	2.743	5.0	0.336	−0.215	505	24.8
600		0.320	1.185	61.8	0.738	2.991	5.4	0.339	−0.072	494	32.8
700		0.346	1.183	55.5				0.360	−0.133	503	44.5
800	8	0.319	1.118	44.9				0.383	−0.236	498	55.1
900		0.272	0.780	35.4				0.354	−0.222	500	64.6
1000		0.297	0.742	33.9				0.350	−0.189	493	66.1
1100		0.261	0.774	32.2				0.362	−0.214	498	67.8
1200		0.365	0.841	35.4				0.353	−0.231	492	64.6
	1	0.313	0.791	71.0	0.947	2.526	5.0	0.342	−0.162	490	24.0
	4	0.322	0.847	66.7	0.860	2.965	3.5	0.365	−0.277	494	27.8
400	8	0.368	0.813	71.4	1.017	2.868	5.1	0.423	−0.262	502	23.5
	12	0.379	0.876	75.3	1.068	2.997	1.7	0.399	−0.139	508	23.0
	16	0.333	0.861	67.9	0.684	2.292	1.2	0.404	−0.238	503	30.9
	1	0.403	1.084	61.5	0.819	2.725	4.2	0.453	−0.142	495	34.5
	4	0.310	1.061	63.3	0.816	2.919	2.3	0.363	−0.186	501	34.4
600	8	0.320	1.185	61.8	0.738	2.991	5.4	0.339	−0.072	494	32.8
	12	0.322	1.197	63.3				0.346	−0.267	502	36.7
	16	0.350	1.119	65.1				0.405	−0.181	508	34.9
	1	0.261	1.114	53.5				0.244	−0.136	506	46.5
	4	0.351	1.061	52.9				0.354	−0.282	494	47.1
800	8	0.284	1.115	46.9				0.377	−0.249	498	53.1
	12	0.260	1.164	47.4				0.287	−0.198	497	52.6
	16	0.322	1.193	45.2				0.366	−0.206	493	54.8
	1	0.295	0.785	38.5				0.364	−0.219	504	61.5
	4	0.191	0.765	35.2				0.294	−0.206	499	64.8
1000	8	0.297	0.742	33.9				0.354	−0.198	493	66.1
	12	0.304	0.761	36.2				0.383	−0.242	503	63.8
	16	0.197	0.753	32.4				0.310	−0.234	497	67.6

* H Unit in k $(1000/4\pi)$ A/m.

There are two main factors to affect Mössbauer parameters during firing process:

(1) The phase transformation of the clay mineral. The clay undergoes four phase transformations in the firing[2~5], shown as Fig. 2.

RT～300℃: dehydration, eliminating the remaining water.

300～800℃: dehydroxylation. The clay mineral lose structural hydroxyls. For example, dehydroxylation of gaolinite leads to a five-fold symmetry for the substitu-

tional iron atom in the original octahedral layer (six-fold symmetry). The gradients of the electric field around iron nucleus increase. This change can be clearly observed in Mössbauer spectrum by a large increase of the ferric quadrupole splitting up to 1.2 mm/s from 0.7 mm/s.

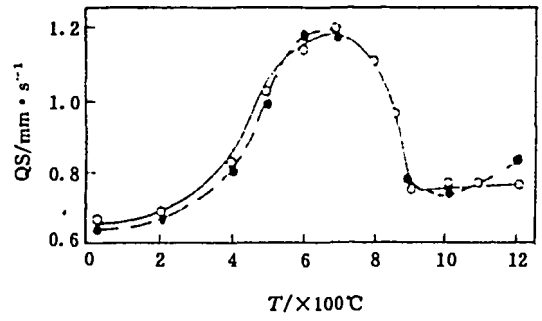

Fig. 2 Fe^{3+} QS values of samples C_1 and C_2 at different temperatures (after 8 h firing)
C_1 —○; C_2 —●

800 ~ 900℃: vitrification. The clay mineral lattice is destroyed. The QS of Fe^{3+} decreases rapidly, from 1.20 to 0.75 mm/s.

900~1200℃: recrystallization. The liquid phase and resolved solid is formed. The new crystal and mineral is formed. These Mössbauer parameters are characteristic parameters of the new mineral, variation being very small. The QS of Fe^{3+} fluctuates near 0.77 mm/s.

(2) The iron minerals transform phases. It is shown as Fig. 3. As temperature increases, the intensity of magnetic peak (M) increases, while intensities of Fe^{3+} and Fe^{2+} decrease. Between 300 and 900℃: the intensity of magnetic peak inceases very fast, while Fe^{3+} intensity decreases rapidly. At 600℃, Fe^{2+} intensity decreases almost to 0. Above 900℃, the intensities of M and Fe^{3+} change slowly. Between 300 and 900℃, all iron minerals take place transformation. For example:

300~450℃: $FeS_2+O_2 \longrightarrow FeS+SO_2$

500~800℃: $4FeS+7O_2 \longrightarrow 2Fe_2O_3+4SO_2$

400℃ and above: γ-$Fe_2O_3 \longrightarrow \alpha$-$Fe_2O_3$

400℃ and above: $2FeOOH \longrightarrow Fe_2O_3+H_2O$

560~750℃: $Fe_2(SO_4)_3 \longrightarrow Fe_2O_3+3SO_3$

800℃: $4FeCO_3+O_2 \longrightarrow 2Fe_2O_3+4CO_2$

From 400℃, various iron minerals tranform to hematite gradually. At the same time, the divalent structural iron ions are oxidized to become trivalent iron ions. The variation can be detected by weakening intensities of Fe^{2+} and Fe^{3+} as well as the increase of the intensities of the magnetic sextets (M). When temperature reaches 800℃ and above, the various iron minerals transform to α-Fe_2O_3. Hence the Mössbauer spectra have sample shapes. The intensities of Fe^{3+} and M change

slowly.

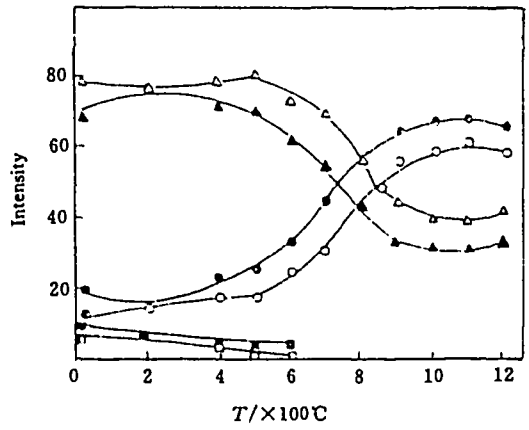

Fig. 3 Intensities of magnetic component (M) and paramagnetic component (Fe^{3+}, Fe^{2+}) of samples C_1 and C_2
C_1 —— M (○); Fe^{3+} (△); Fe^{2+} (□).
C_2 —— M (●); Fe^{3+} (▲); Fe^{2+} (■).

3.1.3 The relations among the parameters and firing time

Fig. 4 shows Fe^{3+} QS values of sample C_1 for different firing temperatures depending on firing time. Fig. 5 shows *M* intensities of sample C_1 depending on firing time. It is not large that the change of QS value of Fe^{3+} vs. firing time and the intensities of *M* vs. firing time. After 8 h of firing, when temperature is particularly higher than 400℃, the QS of Fe^{3+} and *M* intensities are basically constant. When the temperature reaches 400℃ and above, firing time is not main factor which influence on parameters. Especially after 8 h of firing, the parameters are more stable. This is significant to study ancient pottery by means of Mössbauer spectroscopy. As test firing clay and refiring ancient pottery, it is sufficient that to keep constant temperature of 6～8 h at every temperature point.

3.1.4 Determining fired temperature of ancient pottery

Mössbauer parameters of clay, for example Fe^{3+} QS, intensities of various subspectra etc, are functions of firing temperature. Hence according to the Mössbauer parameters of ancient potery the original fired temperature can be estimated. According to QS of Fe^{3+} the firing temperature was usually determined ago. But the QS of Fe^{3+} changes more slowly around 700℃. The Fe^{3+} QS changes also more slowly at 900℃ and above. Therefore the great accuracy cannot be achieved to determine original fired temperature in the temperature range according to QS. The

intensities of Fe^{3+} and magnetic peak M are monotonous function of firing temperature in this temperature range, it is more accurate to determine the temperature by the intensities. Above 900℃, the many Mössbauer parameters of the firing clay are analysed and compared with the refired ancient pottery, and the more accuracy can be got.

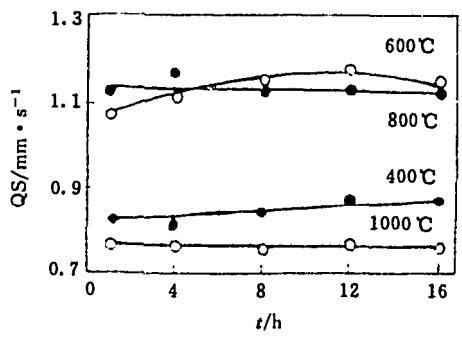

Fig. 4 The relationship between Fe^{3+} QS values of sample C_1 at different firing temperatures and firing times

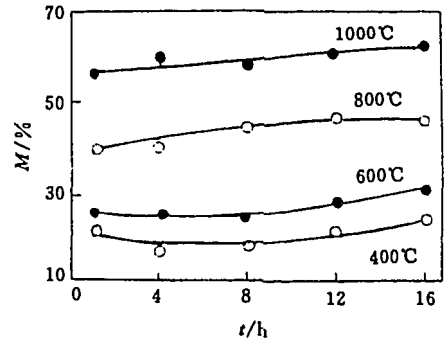

Fig. 5 The relationship between magnetic component intensity (M) of sample C_1 at different firing temperatures and firing times

3.2 The study of the firing process of the sky-green glaze of the imitative ancient Chinese Ru porcelain (IR)

3.2.1 The iron minerals in the sky-green glaze raw material

The Mössbauer spectra of the sky-green glaze at different firing temperatures are shown in Fig. 6. The spectra show that there are three iron minerals: (a) two pairs of paramagnetic doublets of Fe^{2+} and Fe^{3+} in the center of the spectra; (b) a sextet of Fe_2O_3; (c) two sextets of Fe_3O_4. Among the central paramagnetic doublets, a superparamagnetic doublet of iron oxides and the innermost magnetic peaks of Fe_2O_3 and Fe_3O_4 are overlapping. It is difficult to differentiate the paramagnetic doublet in spectra obtained at room temperature. It can only be done with spectra obtained at liquid nitrogen or liquid helium temperatures[1,6,7].

3.2.2 Variation in relative intensities of various iron minerals in sky-green glaze with firing temperature

The variation in the relative intensities of various iron minerals with firing temperature are shown in Fig. 7. Fig. 7 (a) shows that as the temperature increas-

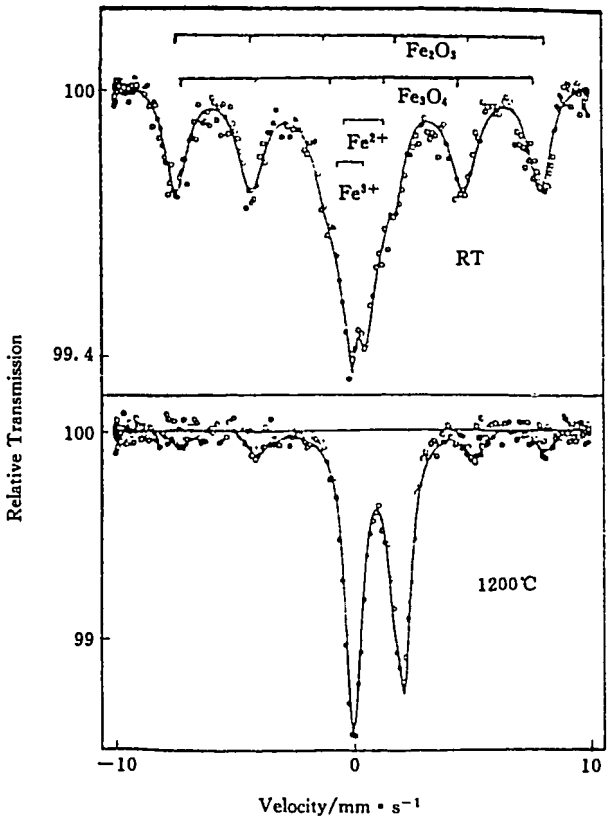

Fig. 6 The Mössbauer spectra of the sky-green glaze raw material at different firing temperature

es, the relative intensity of the paramagnetic peak of Fe^{2+}, i.e. $Fe^{2+}/(Fe^{2+}+Fe^{3+})$, increases slowly at first and then rapidly from 40% to 80% when reaching 700℃. The ratio of the area of the magnetic peak to the overall area is defined as the magnetic ratio. We use (M_1+M_2) to indicate the sum of magnetic ratios of Fe_2O_3 (M_1) and Fe_3O_4 (M_2). The relations of (M_1+M_2) with firing temperature is shown in Fig. 7 (b). As the temperature increases, (M_1+M_2) begins to increase, reaching its maximum near 400℃, and then decreases rapidly. When the temperature is higher than 900℃, the magnetic ratio decreases to 20%.

3.2.3 Phase transition characteristics of sky-green glaze in the firing process

As shown in Fig. 8, there are four characteristic temperature ranges for the phase transition:

(1) Room temperature ~400℃: the glaze eliminates the remaining water and the Mössbauer parameters do not change much.

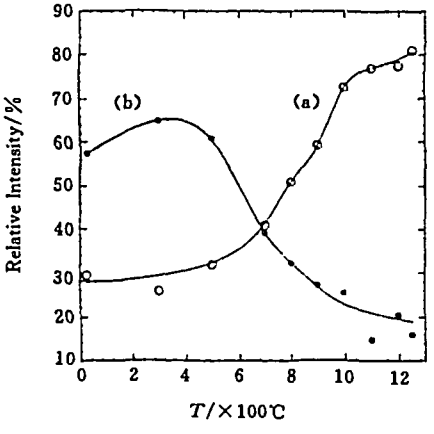

Fig. 7 The variations of $Fe^{2+}/(Fe^{2+}+Fe^{3+})$ of the paramagnetic peak and the magnetic ratio (M_1+M_2) of the sky-green glaze with firing temperature
(a) $Fe^{2+}/(Fe^{2+}+Fe^{3+})$; (b) M_1+M_2.

(2) 400～900℃: the glaze experiences a broad dehydroxylation tempertaure range. The hydroxyls in the lattice get combined to water. The symmetrical distribution of the electrical field around the iron nucleus is destroyed. The gradient of the electric field increases and the QS changes suddenly.

(3) 900～1000℃: as the temperature exceeds 900℃, the glaze is glassified. The mineral lattice is destroyed and a glass state forms. The QS of Fe^{2+} decreases rapidly.

(4) Above 1000℃: the glass state of the glaze emerges. The decomposed substances of the previous minerals recrystallize as new minerals, for example, kaolinite recrystallizes to mullite:

$$2\ [Al_2O_3 \cdot 2SiO_2] \rightarrow \underset{\text{Al-Si spinel}}{2Al_2O_3 \cdot 3SiO_2} + SiO_2 \qquad (950℃)$$

$$3\ [Al_2O_3 \cdot 3SiO_2] \rightarrow 2\ \underset{\text{mullite}}{[3Al_2O_3 \cdot 2SiO_2]} + \underset{\text{critobalite}}{5SiO_2} \qquad (1100℃)$$

In this temperature range, the QS of Fe^{2+} fluctuates near 2.00 and the IS of Fe^{2+} stabilizes at 1.00. These parameters are characteristic of the new mineral.

3.2.4 The coloring mechanism of the sky-green glaze

The appearance of sky-green is closely related to the chemical state of the iron in the glaze. In the high temperature range and reductive atmosphere, Fe_2O_3 and

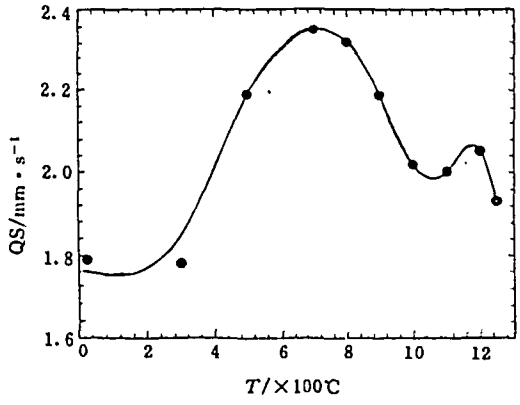

Fig. 8 The relationship between Fe^{2+} QS of the paramagnetic peak of the sky-green glaze and firing temperature

Fe_3O_4 change into FeO:

$$Fe_2O_3+CO \longrightarrow 2FeO+CO_2; \qquad 2Fe_2O_3+C \longrightarrow 4FeO+CO_2$$

$$Fe_3O_4+CO \longrightarrow 3FeO+CO_2; \qquad 2Fe_3O_4+C \longrightarrow 6FeO+CO_2$$

At high temperature, ferrous oxide and silicon oxide become a light-blue glass state substance ($FeO \cdot SiO_2$), and this lays the blue hue for the sky-green Ru porcelain.

For Chinese Ru porcelain, Fe^{2+} and Fe^{3+} ions act as the chief colorant[8]. The Mössbauer spectra in the high temperature range indicate a high concentration of Fe^{2+}. At the firing temperature 1250℃, $Fe^{2+}/(Fe^{2+}+Fe^{3+})$ is 0.81. The particles of the iron distribute evenly in the new material. The sky-green color of Ru porcelain is formed.

3.3 The study of the firing process of the imitative ancient sky-blue Jun porcelain

3.3.1 The iron minerals in the glaze and body materials

The Mössbauer spectra of (IJ_1) and (IJ_2) display magnetic spectra of Fe_2O_3 (M_1) and Fe_3O_4 (M_2), and the paramagnetic spectra of the structural iron. The parameters of Fe^{2+} and Fe^{3+} in the clay mineral lattice (termed structural iron) are very important to trace the phase transformation of clay mineral in the firing process.

3.3.2 The phase transformation of the glaze and body materials in the firing process

Fig. 9 shows the change of the Fe^{2+} quadrupole splitting (QS) of the imitative ancient Jun porcelain glaze with firing temperature. The glaze undergoes dehydration (RT ~ 400℃), dehydroxylation (400 ~900℃), vitrification (900~ 1000℃), and recrystallization (1000~1250℃).

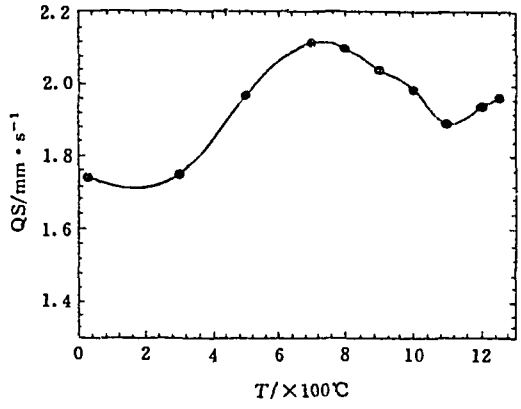

Fig. 9 The relationship between the quadrupole splitting (QS) of Fe^{2+} of the imitative ancient Jun porcelain glaze (IJ_1) and firing temperature (fired for 6 h.)

Fig. 10 shows the change of the Fe^{2+} QS value of the body material with firing temperature. The Fe^{2+} QS value is high from the beginning and increases gradually with the increase of firing temperature. In comparison with the glaze material, the body material does not show clear distinction between dehydration and dehydroxylation. The vitrification temperature range of the body material is relatively low (800 ~1000℃).

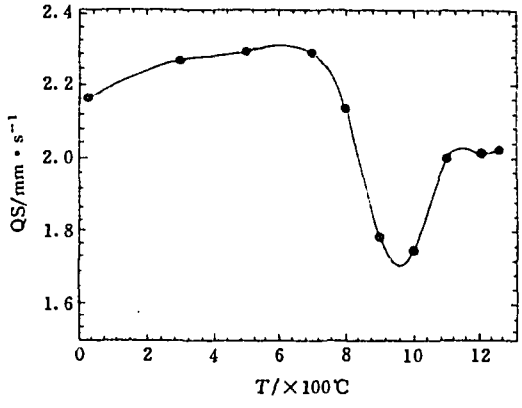

Fig. 10 The relationship between the quadrupole splitting (QS) of Fe^{2+} of the imitative ancient body (IJ_2) and firing temperature (fired for 6 h.)

3.3.3 The changes of various iron intensities in the glaze and body materials

Fig. 11 (a) shows the change of the relative intensity $Fe^{2+}/(Fe^{2+}+Fe^{3+})$ of the paramagnetic peak Fe^{2+} in the glaze with firing temperature. The magnetic ratio (MR) is defined as the ratio of magnetic peak area to the total iron area. The change of the (M_1R+ M_2R) of the glaze material with firing temperature is shown in Fig. 11 (b). As the temperature increases, the $Fe^{2+}/(Fe^{2+}+Fe^{3+})$ increases and (M_1R+M_2R) de-

creases. Fig. 12 shows the relationships between the relative intensity of the paramagnetic peak Fe^{2+}, the magnetic ratio of the body material and firing temperature. Fig. 12 (a) shows that the relative intensity of Fe^{2+} increases rapidly since the firing temperature is above 400℃. It reaches saturation at 900℃, with $Fe^{2+}/(Fe^{2+}+Fe^{3+})$ being 0.79. Fig. 12 (b) shows that the magnetic ratio reaches a maximum at 300℃ and then decreases drastically as the temperature continues to increase. Above 800℃, the magnetic ratio remains at about 0.20. In comparison with the glaze material, it is easier for the newly formed material at high temperature in the body material to capture Fe^{2+} into the lattice.

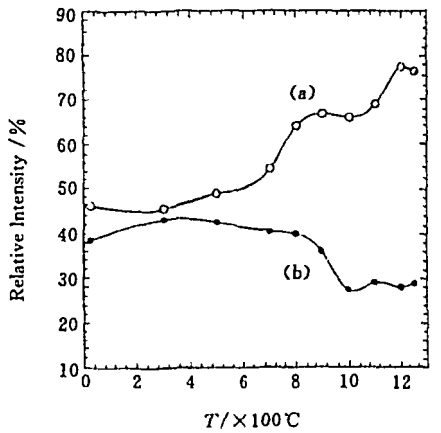

Fig. 11 (a) The relationship between the relative intensity of the Fe^{2+} paramagnetic peak $Fe^{2+}/(Fe^{2+}+Fe^{3+})$ of specimen (IJ_1) and firing temperature. (b) The relationship between the magnetic ratio (M_1R+M_2R) of specimen (IJ_1) and firing temperature

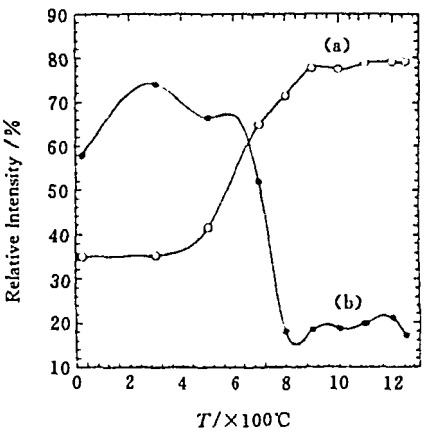

Fig. 12 (a) The relationship between the relative intensity of the Fe^{2+} paramagnetic peak $Fe^{2+}/(Fe^{2+}+Fe^{3+})$ of specimen (IJ_2) and firing temperature. (b) The relationship between the magnetic ratio (M_1R+M_2R) of specimen (IJ_2) and firing temperature

3.3.4 The coloring mechanism

The following changes probably occur in the glaze and body materials when the materials are fired in the reductive atmosphere and high temperature range: the hematite and magnetite transforms ferrous oxide. When FeO distributes in the glass state material of the glaze, the glass state material appears light blue. During the high temperature recrystallization, even more Fe^{2+} ions enter the lattice. This

change can be detected from the obvious increase of the structural iron which has strong effects on glaze color. When Fe^{2+} and Fe^{3+} co-exist, the glaze color is blue. At the firing temperature of 1200℃, the $Fe^{2+}/(Fe^{2+}+Fe^{3+})$ of the glaze of the imitative ancient sky-blue Jun porcelain is 0.75. Fig. 11 (a) indicates that the concentration of Fe^{2+} is very sensitive to the firing temperature. The concentration of reductive atmosphere and firing temperatures are important factors for the coloring of Jun porcelain.

There exist gas bubbles of different sizes in the glaze layer. The broad dehydroxylation and vitrification temperature ranges are beneficial to the formation of these gas bubbles. Vapour, CO_2 and other gases form the bubbles in the glass state glaze layer. The body material contains a lot of Fe_2O_3 and Fe_3O_4, and can produce a large amount of CO_2 gas in the high temperature stage. Observation of the fracture surface of the Jun porcelain glaze layer with a microscope shows that most of the gas bubbles seem to form at the interface between the body and the glaze. This may be related to the CO_2 in the body. These bubbles of different sizes are important factors that lead to the unique opalescence of Jun porcelain[9].

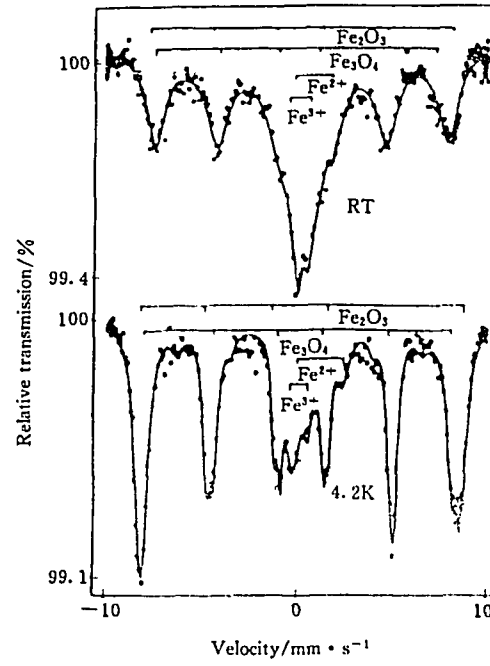

Fig. 13 The Mössbauer spectra of sky-green glaze of imitative ancient Ru porcelain at room temperature and 4.2 K

3.4 Low temperature Mössbauer spectroscopic study on sky-green glaze of imitative ancient Ru porcelain

The Mössbauer spectra of the specimen at RT and 4.2 K are shown as Fig. 13. The Mössbauer parameters of the specimen at RT and 4.2 K are listed in Table 6.

Table 6 Mössbauer Spectrum Parameters of Sky-Green Glaze at Room Temperature and 4.2 K

Temperature	Haematite (Fe_2O_3)				Magnetite (Fe_3O_4)			
T/K	IS/mm·s^{-1}	QS/mm·s^{-1}	H*	I/%	IS/mm·s^{-1}	QS/mm·s^{-1}	H*	I/%
300	0.24	0.00	472	53.5	0.40	0.12	453	12.0
4.2	0.23	0.23	516	60.3	0.19	−0.42	508	19.1

Temperature	Structural (Fe^{2+})				Structural (Fe^{3+})			
T/K	IS/mm·s^{-1}	QS/mm·s^{-1}	W/mm·s^{-1}	I/%	IS/mm·s^{-1}	QS/mm·s^{-1}	W/mm·s^{-1}	I/%
300	1.10	1.91	1.50	9.2	0.24	0.69	1.10	25.3
4.2	1.17	2.46	1.00	7.7	0.13	0.91	0.80	12.9

* Unit in k (1000/4 π) A/m.

3.4.1 The change of the spectrum at 4.2 K

In comparison with the room temperature spectrum, the spectrum at 4.2 K has the following changes:

3.4.1.1 The area of magnetic spectrum increases and the area of paramagnetic spectrum decreases The Mössbauer spectra indicate that haematite (Fe_2O_3) is the major magnetic ordering component, being consistent with the results from X-ray diffraction. In addition, a small amount of magnetite (Fe_3O_4) also exists. One of the most obvious changes of the 4.2 K spectra is that the area of absorption peak of the magnetic ordering component increases while the area of central paramagnetic absorption peak decreases. From room temperature to 4.2 K, the spectrum area of Fe_2O_3 increases from 53.5% to 60.3%, and the spectrum area of Fe_3O_4 increases from 12.0% to 19.1%. In summary, the area of magnetic ordering component increases from 65.5% to 79.3% and the area of paramagnetic peak decreases from 34.5% to 20.6%. The decreases of the paramagnetic peak area of Fe^{3+} is the most prominent, from 25.3% to 12.9%.

3.4.1.2 Intensity of the superfine magnetic field increases At 4.2 K, the superfine magnetic field intensity of the magnetic ordering component increases. For Fe_2O_3, H =472 kOe at 300 K, and H =516 kOe at 4.2 K. For Fe_3O_4, H =453 kOe at 300 K, and H =508 kOe. at 4.2 K.

3.4.1.3 The spectrum widths become narrow The width of the Fe^{3+} paramagnetic doublet peak is 1.10 mm/s at 300 K, and 0.8 mm/s at 4.2 K. The width of the Fe^{2+} paramagnetic peak is 1.5 mm/s at 300 K and 1.00 mm/s at 4.2 K. The widths of all magnetic peaks also generally become narrow.

3.4.1.4 The quadrupole splitting increases The quadrupole splitting (QS) values of structural Fe and magnetic ordering component all increase at 4.2 K. The QS value of structural Fe^{3+} is 0.69 mm/s at 300 K and 0.91 mm/s at 4.2 K. The

QS value of structural Fe^{2+} is 1.91 mm/s at 300 K and 2.46 mm/s at 4.2 K. The QS value of Fe_2O_3 is 0.00 mm/s at 300 K and 0.23 mm/s at 4.2 K. The QS value of Fe_3O_4 changes from 0.12 to −0.42 mm/s.

3.4.2 Analysis and discussion

3.4.2.1 The superparamagnetic relaxation effect of sky-green glaze The particles of haematite and magnetite are superparamagnetic[1,10]. The superparamagnetic relaxation time of these microcrystalline particles is determined by the following formula:

$$\tau = \tau_0 \exp(KV/kT) \tag{1}$$

where K is the anisotropic constant, V the volume of magnetic domain, kT the thermal energy. The superparamagnetic relaxation time depends strongly on temperature and particle size. If the time is long (large V, small T), the system is ferromagnetic. Mössbauer spectrum shows Zeeman splitting spectrum. If the time is short (small V, large T), the system is paramagnetic, and Mössbauer spectrum is paramagnetic. At room temperature (far below Neel temperature), the Mössbauer spectrum contains both Zeeman splitting and paramagnetic component, due to the superparamagnetic relaxation effect of sky-green glaze. The area ratio of the two components is 66 : 34. The paramagnetic peak of the room temperature spectrum is the result of the superposition of the paramagnetic peaks of Fe_2O_3 and Fe_3O_4 and the paramagnetic peaks of structural Fe. It is difficult to differentiate these two kinds of spcetra at room temperature, while the paramagnetic effect does not exist at 4.2 K. Therefore the paramagnetic peaks of Fe oxides disappear, and the Zeeman splitting component increases. The paramagnetic peak of spectrum at 4.2 K is completely due to the Fe particles that already exist in the clay mineral structure. The area ratio of the magnetic peak and paramagnetic peak is 79 : 21 at 4.2 K.

3.4.2.2 Enlightenment to coloring mechanisms of Green Porcelain The relative abundance of various states of Fe in the glaze can be determined by Mössbauer spectroscopy, which by itself is significant to the study of scientific and technological problems of porcelains. Chemical analysis and X-ray diffraction indicate only Fe_2O_3 as the Fe mineral in sky-green glaze. However, the Mössbauer spectra at 4.2 K reveal that there are haematite, magnetite and structural Fe (Fe^{2+}, Fe^{3+}) in sky-green glaze. Their relative abundences are 60% for Fe_2O_3, 19% for Fe_3O_4, 13% for Fe^{3+} and 7.7% for Fe^{2+}. The superparamagnetic percentage of ferric oxide particles is the function of temperature. Hence the size distribution of ferric oxide parti-

cles can be calculated. The coloring of the glaze is related to the abundence and size of ferric oxide particles, as well as the abundence of structural Fe. The abundence of various Fe and particle size are determined by the firing temperature and atmosphere. For the same glaze material, different glaze color results from different firing conditions. Therefore it is not possible to determine the chemical state of Fe in detail by chemical analysis and X-ray diffraction, and the usage of Mössbauer spectroscopy in the study of ancient porcelains shows the unique advantage.

3. 4. 2. 3 The reasons for the change of other superfine parameters

(1) The increase of the room temperature spectrum width

There are many reasons for the increase of spectrum width. The major two reasons under our experimental condition are:

(i) The diffusion movement of atoms

The formula for the spectrum width increase is[11]

$$\triangle\Gamma = 2h/\tau_0[1 - 1/(1 + k^2\langle\alpha_0^2\rangle/6\tau)] \qquad (2)$$

The higher the temperature is, the larger the average square value $\langle\alpha_0^2\rangle$ of the migration distance, the shorter the staying time τ_0 at a position and the bigger the spectrum width $\triangle\Gamma$.

(ii) Superparamagnetic relaxation effect. The higher the temperature is, the more prominent the superparamagnetic relaxation effect of haematite and magnetite particles is and the more the spectrum widens.

(2) The increase of quadrupole splitting value of low temperature spectrum

One possible explanation for this result is as follows.

Under thermal equilibrium conditions, the arrangement of atoms at various energy levels follows Boltsmann distribution, i. e.

$$N_i = g_i\exp(-E_i/KT) \qquad (3)$$

The number of atoms at one energy level, N_i, is determined by the energy E_i and temperature. It is obvious that the lower the temperature is, the larger the number of atoms at low energy states, and the closer the maximum of valence electron cloud density of atom at low energy states to the nuclei, which make the electric charge distribution of inner electron shell more asymmetrical. The gradient of the electric field resulting from the polarization induction of inner electron shells near the nuclei is larger. Therefore, the increase of quadrupole splitting value is experimentally observed at low temperature.

REFERENCES

[1] Gangas N H, et al. Clays and Clay Minerals, 1973, (21): 151~160

[2] Maniatis Y, Simopoulos A, Kostikas A. Am. Ceram. Soc., 1983, (66, 11): 773
[3] Chevalier R, Coey J M D, Bouchez R. J. de Phys., 1976, (C6): 861
[4] Simopoulos A, Kostikas A, et al. Clays and Clay Minerals, 1975, (23): 393
[5] Janot C, Deleroix P. J. de Phys., 1974, (C6): 557
[6] Kostikas A, Simopoulos A, Gangas N H. J. de Phys., 1974, (C1): 107
[7] Chen Songhua, Gao Zhengyao, Sun Zhongtian. Chinese Science Bulletin, 1994, (3): 204
[8] Li Jiazhi, Chen Xianqiu (eds.) The Science and Technology of Ancient Ceramic 1. proc. Int. Conf. Scientific and Technological Literature Publ. Shanghai, (1992): 266～271
[9] Chen Xiaqiu, et al. Chinese J. Silicate, 1983, (11): 129
[10] Cohen R L. Applications of Mössbauer spectroscopy, 1980, 11: 1～48
[11] Xia Yuanfu, Ye Chunjing, Zhang Jian. Mössbauer Effect and its Application (in Chinese) Atomic Energy Publishing Company, Beijing: 1884, 114

（京）新登字 077 号

图书在版编目（CIP）数据

粘土和仿古瓷的穆斯堡尔实验＝THE MÖSSBAUER EXPERIMENT ON THE CLAYS AND THE IMITATIVE ANCIENT PORCELAINS/高正耀等著. －北京：原子能出版社，1995. 12

Ⅰ. 粘… Ⅱ. 高… Ⅲ. ①核技术-研究报告-中国②粘土-瓷器-穆斯堡尔效应 Ⅳ. ①TL-24②TL993

中国版本图书馆 CIP 数据核字（95）第 11055 号

原子能出版社出版发行

责任编辑：孙凤春

社址：北京市海淀区阜成路 43 号 邮政编码：100037

中国核科技报告编辑部排版

核科学技术情报研究所印刷

☆

开本 787×1092 1/16 · 印张 1/2 · 字数 21 千字

1995 年 12 月北京第一版 · 1995 年 12 月北京第一次印刷

CHINA NUCLEAR SCIENCE & TECHNOLOGY REPORT